that there is essentially no difference in the shapes of the ^{35}Cl signal between samples that contain no I^- cavities, Figure 10a,c, and sodalite matrices which contain a relatively high abundance of I^- anions, Figure 10b,d. This result is different from the shape sensitivity of the ^{81}Br MAS resonance to anion-empty cavities, Figure 2, which again might indicate that imbibed water molecules in the anion-empty cages have a significant nearest-neighbor effect on the shape of the NMR signal.

However, there is a noticeable change in the *positions* of the ^{35}Cl peaks as I^- anions are distributed in the sodalite lattice. The ^{35}Cl signal, ascribed to encapsulated Na_4Cl tetrahedra, shifts from −122 ppm, Figure 10a, to −125 ppm, Figure 10b, as most of the cavities become occupied with I^- anions. In a similar way, the ^{35}Cl peak, which is ascribed to coupled Ag_4Cl tetrahedra, shifts from −310 ppm, Figure 10c, to −305 ppm, Figure 10d, in the samples that contain 100% and 27% Cl^- anions in the sodalite lattice, respectively. Note that the position of the ^{35}Cl peak from $Ag_8Cl_{0.46}I_{1.54}$–sodalite, Figure 10d, is observed farther *downfield*, relative to the ^{35}Cl peak which arises from Ag_8Cl_2–sodalite, Figure 10c. This relative shift is opposite to the corresponding ^{35}Cl positions, at −125 ppm and −122 ppm, respectively, *before* the Ag^+ exchange, Figure 10b,a.

The unit-cell size of $Na_{8-n}Ag_nCl_{2-m}I_m$–sodalite enlarges with a higher iodide content.[23] Therefore, in the $Na_8Cl_{2-m}I_m$–sodalites, the Na_4Cl clusters experience an enhanced ionicity in the Na_4I-rich sodalite lattice, resulting in a more localized negative charge on the Cl^- anions and the observed upfield shift of 3 ppm, Figure 10a,b. By contrast, the outcome of placing the Ag_4Cl tetrahedra in an increasingly rich Ag_4I lattice could be to slightly change the intracavity interaction between the Ag^+ cation and the Cl^- anion, leading to deshielding of the ^{35}Cl nuclei and the observed downfield shift of 5 ppm, Figure 10c,d.

Conclusions

^{81}Br and ^{35}Cl MAS experiments conducted on silver-exchanged sodium,halo–sodalites yield useful information on the environments of encapsulated clusters within the sodalite lattice. Na_4X (X = Br, Cl) tetrahedra provide a symmetrical environment around the halide anion and give rise to narrow resonances at specific locations in the ^{81}Br and ^{35}Cl MAS spectra. The shape of the ^{81}Br peaks displays a sensitivity toward the distribution of anion-empty cavities within the sodalite matrix, while the positions of the corresponding ^{35}Cl signals exhibit a similar sensitivity to I^--containing cavities. Spin–lattice and spin–spin relaxation measurements provide insight into interactions which involve the ^{81}Br nuclei, as well as motional aspects of the encapsulated clusters.

A strong shielding of the ^{81}Br and ^{35}Cl nuclei is detected, following Ag^+-cation exchange, in sodalite lattices where interaction between adjacent Ag_4Br and Ag_4Cl clusters, respectively, is facilitated. The upfield signal is not detected in samples that contain a high abundance of anion-empty cavities, relative to Br^--containing cavities. A percolation threshold is observed in a sodalite sample with an intermediate ratio of Br^--containing to Br^--empty cavities.

Acknowledgment. This work was supported by the Director, Office of Energy Research, Office of Basic Energy Sciences, Materials and Chemical Sciences Division, U.S. Department of Energy, under Contract No. DEAC03-76SF00098. R.J. is grateful to Professor A. Pines, Dr. J. Haase, and T. Hanna for helpful discussions. G.A.O. wishes to acknowledge the Natural Sciences and Engineering Research Council (NSERC) of Canada's Operating and Strategic Grants Programmes. A.S. would like to thank NSERC for a 1967 Science and Engineering Postgraduate Scholarship.

Poly(arylmethyl) Quartet Triradicals and Quintet Tetraradicals[1]

Andrzej Rajca* and Suchada Utamapanya

Contribution from the Department of Chemistry, University of Nebraska, Lincoln, Nebraska 68588. *Received August 20, 1992*

Abstract: Three poly(arylmethyl) quartet triradicals and three quintet tetraradicals are prepared by oxidation of the corresponding carbanions. The ground states for polyradicals in frozen solutions are established using ESR spectroscopy (4–100 K), including Curie plots (10–80 K), and SQUID magnetometry (2–80 K). For two triradicals and one tetraradical, ESR $\Delta m_s = 2$ transitions are resolved; for one triradical, the $\Delta m_s = 3$ transition is observed. The *i*-Pr-substituted triradical and tetraradical are isolated as solids and studied using SQUID; thermal population of low spin states is negligible at ambient temperature. The most intense bands in the UV–vis spectra for *i*-Pr-substituted tri- and tetraradicals are similar to those found in the homologous diradicals. Electrochemical study of the *i*-Pr-substituted triradical at 195–200 K reveals three reversible voltammetric waves (peaks) that correspond to three one-electron reductions to the corresponding trianion.

Introduction

High-spin organic molecules are closely related to the recent topics of organic magnetism.[2-7] Molecules with many unpaired electrons, which possess high-spin ground states preferred by large margin and stable at ambient temperature, are particularly

(1) This research project was initiated at Kansas State University.

(2) High spin may be defined as parallel alignment of spins for all available unpaired electrons such as $S \geq {}^1/_2$.

(3) For reviews, see: *Proceedings of the Symposium on Ferromagnetic and High Spin Molecular Based Materials*; 197th National Meeting of the American Chemical Society, Dallas, Texas. Miller, J. S.; Dougherty, D. A. *Mol. Cryst. Liq. Cryst.* **1989**, *176*, 1–562. Buchachenko, A. L. *Russ. Chem. Rev.* **1990**, *59*, 307. Iwamura, H. *Adv. Phys. Org. Chem.* **1990**, *26*, 179. Dougherty, D. A. *Acc. Chem. Res.* **1991**, *24*, 88.

(4) High-spin poly(arylmethyl) polyradicals ($S = 2$–5): (a) Rajca, A.; Utamapanya, S.; Thayumanavan, S. *J. Am. Chem. Soc.* **1992**, *114*, 1884. (b) Rajca, A. *J. Am. Chem. Soc.* **1990**, *112*, 5889. (c) Rajca, A. *J. Am. Chem. Soc.* **1990**, *112*, 5890.

(5) High-spin tetraradicals: (a) Seeger, D. E.; Berson, J. A. *J. Am. Chem. Soc.* **1983**, *105*, 5144, 5146. (b) Seeger, D. W.; Lahti, P. M.; Rossi, A. R.; Berson, J. A. *J. Am. Chem. Soc.* **1986**, *108*, 1251. (c) Berson, J. A. In *The Chemistry of Quinoid Compounds*; Patai, S., Rappaport, Z., Eds.; Wiley: New York, 1988; Vol. II, Chapter 10. (d) Novak, J. A.; Jain, R.; Dougherty, D. A. *J. Am. Chem. Soc.* **1989**, *111*, 7618. (e) Dougherty, D. A. *Mol. Cryst. Liq. Cryst.* **1989**, *176*, 25.

0002-7863/93/1515-2396$04.00/0

challenging and promising targets for the following two approaches to organic magnets.

In the first approach, the control of the molecular shape and intramolecular magnetic interactions may lead to a synthesis of a single-molecule nanometer-size magnetic particle which would possess a single magnetic domain.[8,9] The high spin for a large number of electrons is essential. Reports of series of high-spin polycarbenes (S = 2–6) and polyradicals (S = 2–5) may be viewed as initial steps in this direction.[4,7]

In the second approach, the control of intermolecular magnetic interactions is important; high-spin molecules are the building blocks of a molecular solid. If a simple mean-field theory is applicable to magnetic interactions between high-spin organic molecules, then the higher spin (S) values for the component molecules should provide higher transition temperatures to ferromagnetism (Curie temperature, T_C) according to the following relationship: $T_C \propto S(S+1)$.[10] Several reports of weak intermolecular ferromagnetic interactions in the liquid helium temperature range for mono- and diradicals and phase transitions to ferromagnets with Curie temperatures, T_C = 0.6 K, for monoradicals have appeared.[11,12]

Thermal stability of high-spin molecules is obviously useful for convenient handling of materials. Furthermore, it allows the measurement of a wide range of energy differences between the states of various spin by detecting thermal population; such measurements are essential to the understanding of the ferro- vs. antiferromagnetic spin coupling.

Recent reports aimed at stable high-spin systems find lack of or little preference for high spin in stable di- and trinitroxides.[13] 1,3-Connected poly(arylmethyl) diradicals, which are highly sterically hindered, are thermally stable and show large preference for a triplet ground state.[14] The important questions are as follows: (1) Can thermally stable tri- and tetraradicals with large preference for the high-spin ground state be made? (2) Is the planarity of π-conjugated systems of polyradicals necessary for significant ferromagnetic coupling between unpaired electrons?

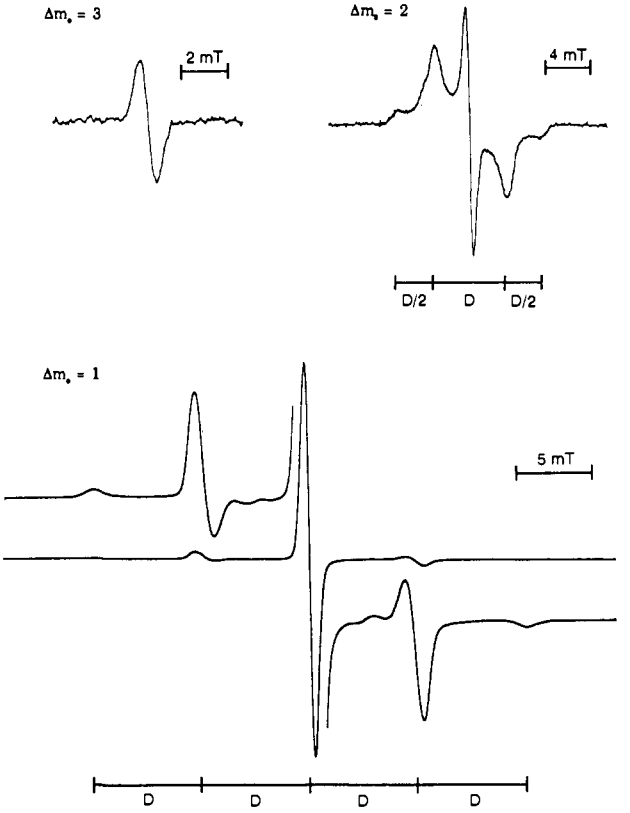

Figure 1. X-band ESR spectrum for Me-substituted triradical **2** in THF/2-MeTHF glass. Upper left: Δm_s = 3 region at 4 K. Upper right: Δm_s = 2 region at 4 K. Bottom: Δm_s = 1 region at 100 K.

In the preliminary communication, we have reported poly(arylmethyl) quintet tetraradical **4**, which was persistent in solution at low temperatures.[4c] Now, we determine the ground state for

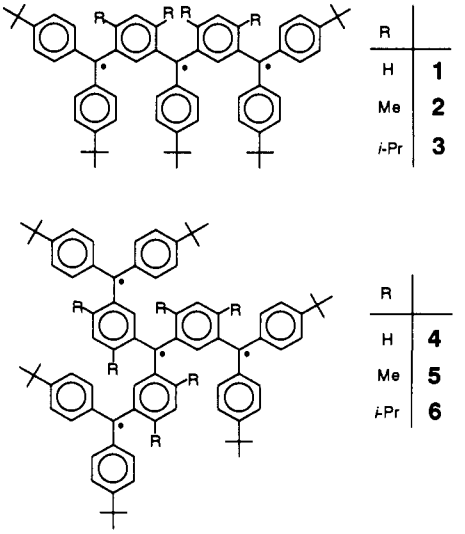

4 and describe a series of the related high-spin triradicals **1–3** and tetraradicals **5** and **6**. The most sterically hindered triradical **3** and tetraradical **6** are isolated as solids and show no detectable thermal population of the low-spin states at ambient temperature.

Results and Discussion

Preparation of Tri- and Tetraradicals. Tri- and tetraradicals are obtained by treatment of their ether precursors with lithium metal in tetrahydrofuran (THF),[4b,15] followed by oxidation of

(6) High-spin triradicals: (a) Yoshizawa, K.; Chano, A.; Ito, A.; Tanaka, K.; Yamabe, T.; Fujita, H.; Yamauchi, J.; Shiro, M. *J. Am. Chem. Soc.* **1992**, *114*, 5994. (b) Veciana, J.; Rovira, C.; Armet, O.; Domingo, V. M.; Crespo, M. I.; Palacio, F. *Mol. Cryst. Liq. Cryst.* **1989**, *176*, 77. (c) Weissman, S. I.; Kothe, G. *J. Am. Chem. Soc.* **1975**, *97*, 2538. (d) Brickmann, J.; Kothe, G. *J. Chem. Phys.* **1973**, *59*, 2807. (e) Kothe, G.; Ohmes, E.; Brickmann, J.; Zimmermann, H. *Angew. Chem., Int. Ed. Engl.* **1971**, *10*, 938. Schmauss, G.; Baumgartel, H.; Zimmermann, H. *Angew. Chem., Int. Ed. Engl.* **1965**, *4*, 596.

(7) High-spin polycarbenes (S = 2–6): Nakamura, N.; Inoue, K.; Iwamura, H.; Fujioka, T.; Sawaki, Y. *J. Am. Chem. Soc.* **1992**, *114*, 1484. Fujita, I.; Teki, Y.; Takui, T.; Kinoshita, T.; Itoh, K.; Miko, F.; Sawaki, Y.; Iwamura, H.; Izuoka, A.; Sugawara, T. *J. Am. Chem. Soc.* **1990**, *112*, 4074. Sugawara, T.; Bandow, S.; Kimura, K.; Iwamura, H.; Itoh, K. *J. Am. Chem. Soc.* **1984**, *106*, 6449. Sugawara, T.; Bandow, S.; Kimura, K.; Iwamura, H.; Itoh, K. *J. Am. Chem. Soc.* **1986**, *108*, 368. Takui, T.; Itoh, K. *Chem. Phys. Lett.* **1973**, *19*, 120. Itoh, K. *Chem. Phys. Lett.* **1967**, *1*, 235. Wasserman, E.; Murray, R. W; Yager, W. A.; Trozzolo, A. M.; Smolinsky, G. *J. Am. Chem. Soc.* **1967**, *89*, 5076.

(8) (a) Rajca, A.; Utamapanya, S. In the proceedings from the International Symposium on Chemistry and Physics of Molecular Based Magnetic Materials, Tokyo, Japan, October 1992; to be published in *Mol. Cryst. Liq. Cryst.* (b) Rajca, A. In *Advances in Dendritic Molecules*; Newkome, G. R., Ed.; JAI Press: Greenwich; Vol. 1, in press.

(9) Nanometer-size antiferromagnetic and ferromagnetic particles: Awschalom, D. D.; DiVincenzo, D. P.; Smyth, J. F. *Science* **1992**, *258*, 414 and references therein.

(10) (a) Mean-field: Carlin, R. L. *Magnetochemistry*; Springer-Verlag: Berlin, 1986. (b) The $T_C \propto S(S+1)$ relationship may be applicable to solids based upon molecules with similar size and structure but different spin (S).

(11) Ferromagnetic interactions in organic solids: ref 14a and references therein.

(12) Organic ferromagnet: Kinoshita, M.; Turek, P.; Tamura, M.; Nozawa, K.; Shiomi, D.; Nakazawa, Y.; Ishikawa, M.; Takahashi, M.; Awaga, K.; Inabe, T. Maruyama, Y. *Chem. Lett.* **1991**, 1225. Tamura, M.; Nakazawa, Y.; Shiomi, D.; Nozawa, K.; Hosokoshi, Y.; Ishikawa, M.; Takahashi, M.; Kinoshita, M. *Chem. Phys. Lett.* **1991**, *186*, 401.

(13) Matsumoto, T.; Koga, N.; Iwamura, H. *J. Am. Chem. Soc.* **1992**, *114*, 5448. Dvolaitzky, M.; Chiarelli, R.; Rassat, A. *Angew. Chem., Int. Ed. Engl.* **1992**, *31*, 180. Ishida, T.; Iwamura, H. *J. Am. Chem. Soc.* **1991**, *113*, 4238. Calder, A.; Forrester, A. R.; James, P. G.; Luckhurst, G. R. *J. Am. Chem. Soc.* **1969**, *91*, 3724.

(14) (a) Rajca, A.; Utamapanya, S.; Xu, J. *J. Am. Chem. Soc.* **1991**, *113*, 9235. (b) Veciana, J.; Rovira, C.; Crespo, M. I.; Armei, O.; Domingo, V. M.; Palacio, F. *J. Am. Chem. Soc.* **1991**, *113*, 2552. (c) Rajca, A.; Utamapanya, S. *J. Org. Chem.* **1992**, *57*, 1760.

0.015–0.06 M solutions of carbanions in THF with 1.5 or 2 molar equiv of iodine at $T \leq 195$ K.[4a,c] For ESR spectroscopy, the THF solutions of tri- and tetraradicals are diluted with 2-methyltetrahydrofuran (2-MeTHF) at low temperature.[4a]

For preparation of solid triradical **3** and tetraradical **6**, the corresponding carbanions are obtained in THF and, then, solvent is changed from THF to Me_2O. After oxidation at low temperature, Me_2O is removed at 195 K under vacuum, the remaining residue is repeatedly treated with degassed MeOH, and, then, dried under high vacuum. **3** and **6**, which are light yellow-green solids, are stored under argon in the glovebox refrigerator. Solid **3** and **6** are persistent at ambient temperature over a few days; in solution, decomposition is detectable after a short period.

Triradicals: ESR Studies in Solution. The $\Delta m_s = 1$ regions of the ESR spectra for triradicals in 2-MeTHF/THF at 100 K consist of several (**1**) or primarily five (**2** and **3**) symmetrical peaks; the center peaks are the most intense by far (Figure 1).[26] The spectra for **2** and **3** are assigned to quartet states with the zero-field splitting (zfs) parameters, $|E/hc| \approx 0$ and $|D/hc| = 0.0066$ cm^{-1} (**2**) and $|D/hc| = 0.0069$ cm^{-1} (**3**); the theoretical spectrum for such quartet states should possess five symmetrical peaks equally spaced by $|D/hc|$ and with the center peak possessing the dominant peak-to-peak height.[6c,18] For **2**, additional weak resonances are also observed (Figure 1). One of the possible, but not unique, assignments for the spectrum of **1** might be two quartets (e.g., $|E/hc| = 0$, $|D/hc| = 0.0057$ cm^{-1} and $|E/hc| = 0.0004$ cm^{-1}, $|D/hc| = 0.0043$ cm^{-1}). The extraneous peaks in the ESR spectra of **2** and two sets of peaks assigned to quartets for **1** suggest that the isomeric species may be present for these two triradicals in the 2-MeTHF/THF matrix.

At 4 K, intense ESR spectra in the $\Delta m_s = 1$ region are observed for **2** and **3**.[16] Notably, resolved spectra are also found at lower magnetic fields ($\Delta m_s = 2$ and 3 regions, Figure 1). For **1**, two broad side lines are found in the $\Delta m_s = 2$ region at 4 K;[26] a narrow center peak is assigned to a triplet impurity. This partial resolution of the quartet $\Delta m_s = 2$ region is consistent with spectral overlap of more than one quartet species for **1** as found in the $\Delta m_s = 1$ region. For **2** at 4 K and **3** at 11 K, four broad lines with $|D/2hc|$, $|D/hc|$, $|D/2hc|$ spacings are found in the $\Delta m_s = 2$ region which indicates one quartet;[26] a narrow center peak is assigned to a triplet impurity.[17a] For **2**, one narrow line at the third field ($\Delta m_s = 3$) is observed at 4 K (Figure 1).[17b] These $\Delta m_s = 2, 3$ spectra for quartet triradical **2** show a qualitative resemblance to the $\Delta m_s = 1, 2$ spectra of a triplet with half the $|D/hc|$ value. These data unequivocally establish the quartet ground state for **2** and suggest that **1** and **3** are quartets ($S = {}^3/_2$). These results are confirmed for **3** by SQUID studies in the solid state (following text).

Tetraradicals: ESR and SQUID Studies in Solution. For tetraradical **4**, eight symmetrical lines are observed in the $\Delta m_s = 1$ region of the ESR spectrum in 2-MeTHF/THF at 100 K; the line in the center corresponds to a half-integral spin impurity (Figure 2). The resolution is significantly improved compared to the original spectrum of **4** in THF.[4c] Computer simulation ($\Delta m_s = 1$) suggests a quintet with $|E/hc| \approx 0$ cm^{-1} and $|D/hc| = 0.00300$ cm^{-1} (Figure 2).[18] A similar eight-line ESR spectrum is obtained for **5**; however, the lines are broader and $|D/hc| \approx 0.0021$ cm^{-1} (Figure 3). Presumably, more than one quintet species with similar zfs parameters contribute to the spectrum or/and $|E/hc|$ is not exactly null. For **6**, the ESR spectrum in the $\Delta m_s = 1$ region is complex;[26] at least two quintets (isomers) with different zero-field parameters are present.[19] The peak-to-peak heights of the center peak (a half-integral spin impurity) relative to the quintet

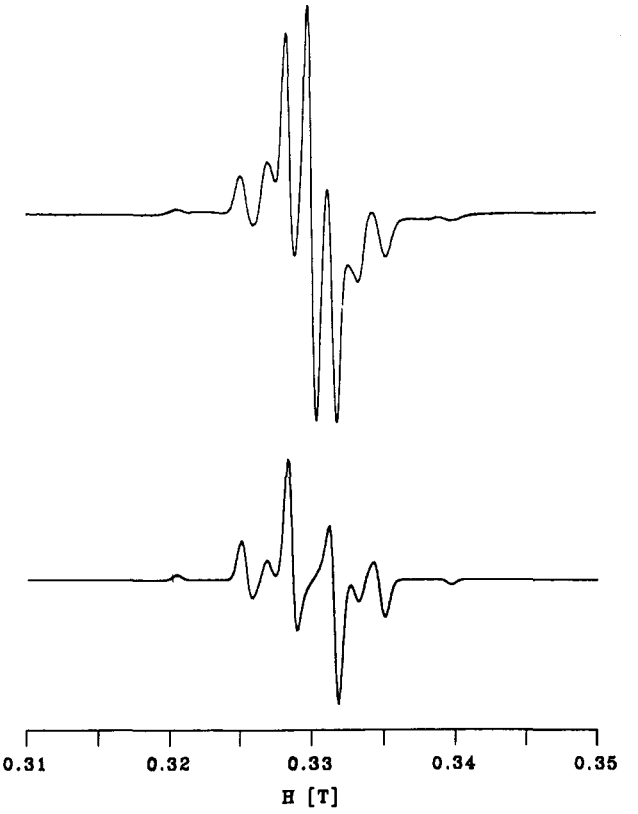

Figure 2. Top: X-band ESR spectrum in the $\Delta m_s = 1$ region for tetraradical **4** in THF/2-MeTHF glass at 100 K. Bottom: Simulated $\Delta m_s = 1$ spectrum using a Gaussian line width of 6 G and quintet zfs, $|D/hc| = 0.00300$ cm^{-1} and $|E/hc| \approx 0$ cm^{-1}.

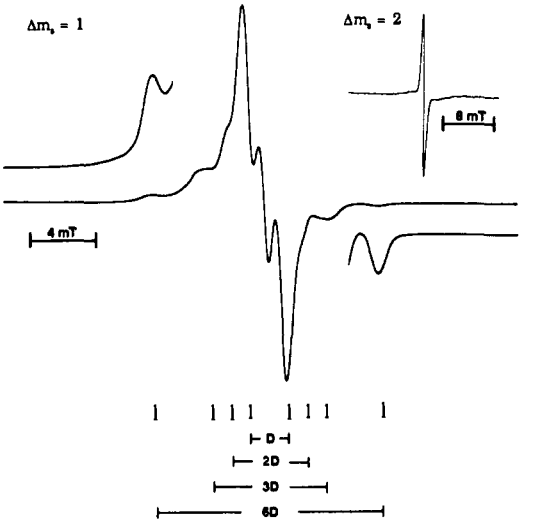

Figure 3. X-band ESR spectrum in the $\Delta m_s = 1$ region for tetraradical **5** in THF/2-MeTHF glass at 4 K. The line spacings are expressed in terms of "D" for quintet state with $E \simeq 0$ cm^{-1}. Insert: $\Delta m_s = 2$ region at 4 K.

(15) (a) Utamapanya, S.; Rajca, A. *J. Am. Chem. Soc.* **1991**, *113*, 9242. (b) Rajca, A. *J. Org. Chem.* **1991**, *56*, 2557. (c) Synthesis of the precursor polyether for tri- and tetraradicals **1–3**, **5**, **6**: Rajca, A.; Janicki, S., manuscript in preparation.

(16) For **1** the ESR spectrum in the $\Delta m_s = 1$ region was severely distorted at low temperatures even at the highest available microwave power attenuation settings (lowest power).

(17) (a) The previous observations of the $\Delta m_s = 2$ transitions for $S = {}^3/_2$ systems failed to resolve the four peaks for $|E/hc| \approx 0$ quartets; ref 6a,c. (b) This is the first observation of a $\Delta m_s = 3$ transition at X-band for an $S = {}^3/_2$ triradical. The instrument settings for the $\Delta m_s = 2$ and 3 transitions shown in Figure 1 are as follows; microwave power, 0.82 mW, 13.0 mW; modulation amplitude, 0.25 mT, 0.40 mT; receiver gain, 5.0×10^5, 6.3×10^5; the peak-to-peak height of both transitions steadily increases with microwave power up to our highest power setting of 206 mW; the other settings are identical for both regions. The intensity of the observed $\Delta m_s = 3$ line is larger than predicted in ref 6c; i.e., the ratio of the $\Delta m_s = 2, 3$ transitions in **2** is significantly less than $(H/D)^2 \approx 2000$ which is helpful for the detection of the $\Delta m_s = 3$ transition.

(18) Computer simulation of ESR spectra for high-spin systems: Thayumanavan, S.; Rajca, A., unpublished work. Teki, Y.; Takui, T.; Itoh, K. *J. Chem. Phys.* **1988**, *88*, 6134. Teki, Y.; Takui, T.; Yagi, H.; Itoh, K. *J. Chem. Phys.* **1985**, *83*, 539. Iwasaki, M. *J. Magn. Reson.* **1974**, *16*, 417.

(19) Propeller isomerism; Mislow, K. *Acc. Chem. Res.* **1976**, *9*, 26.

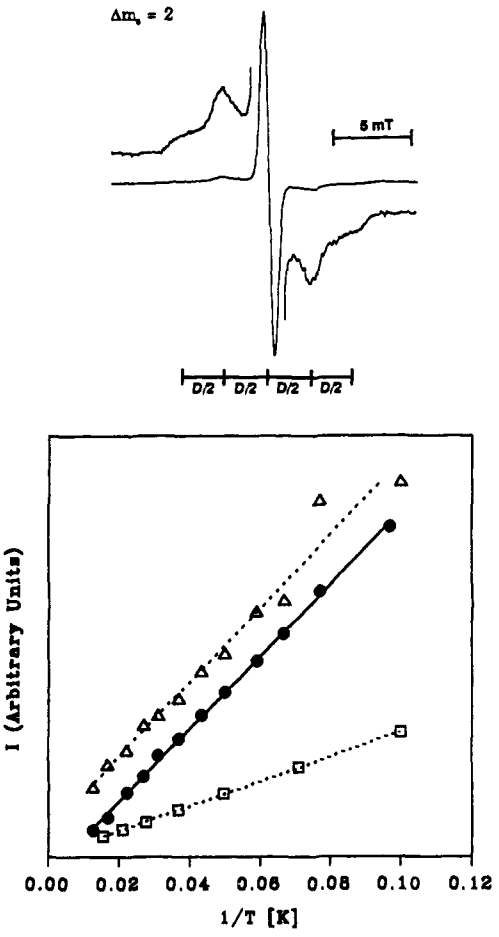

Figure 4. Top: X-band ESR spectrum in the $\Delta m_s = 2$ region for tetraradical **4** in THF/2-MeTHF glass at 4 K. The line spacings are indicated in terms of "D" as shown in the figure. Bottom: ESR Curie plots for tetraradicals **4** (triangles), **5** (squares), and **6** (solid circles); intensity (I) of the center resonance in the $\Delta m_s = 2$ region vs. inverse of the temperature ($1/T$) in the 10–80 K range (**4** and **6**) and 10–65 K range (**5**).

resonances for **5** and **6** are significantly less compared to **4** (Figures 2 and 3).[20,26]

ESR studies at cryogenic temperatures reveal intense spectra in the $\Delta m_s = 1$ region for all three tetraradicals at 4 K (e.g., Figure 3). In the $\Delta m_s = 2$ region, all three tetraradicals show an intense center peak and the underlying broad feature (e.g., Figure 3). For **4**, which possesses relatively large $|D/hc|$, a symmetrical spectrum consisting of five peaks with $|D/2hc|$ separations is resolved at 4 K.[21] The center peak is relatively intense and narrow compared to the weak and broad side peaks (Figure 4). Thus, the $\Delta m_s = 2$ spectrum for quintet tetraradical **4** qualitatively resembles a $\Delta m_s = 1$ region for a quartet with half the $|D/hc|$ value. Because of the small value of $|D/hc|$ for **5** and the presence of isomers for **6**, only the center peak can be identified in the $\Delta m_s = 2$ region for these two tetraradicals.[21]

The ESR intensities (I) of the $\Delta m_s = 2$ center peaks are studied as a function of temperature in the 4–80 K (4–65 K for **5**) temperature range. For $|E/hc| = 0$ spin systems with 1–4 unpaired electrons, only quintet and triplet states may contribute to this peak. The Curie plots, i.e., I vs. $1/T$, are linear in the 10–80 K temperature range (Figure 4). AT $T < 10$ K, a slight curvature in the plot can be observed which may originate in microwave saturation effects[5c] or onset of antiferromagnetic interactions.

(20) The center lines, which may correspond to a doublet ($S = {}^1/_2$) spectrum or "xyz" transition for quartet ($S = {}^3/_2$) species, when compared to other lines corresponding to high-spin species, are relatively narrow and intense in the media such as frozen solutions; therefore, the amount of the half-integral spin impurities as judged by the height of the center peak is small.

(21) A complicated $\Delta m_s = 2$ spectrum was observed for a $|E/hc| \neq 0$ quintet, see ref 5d.

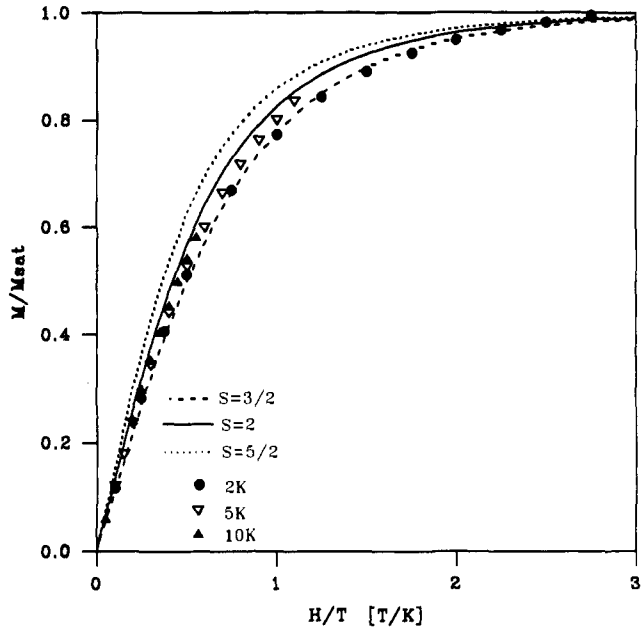

Figure 5. Normalized plots of magnetization vs. ratio of magnetic field and temperature (M/M_{sat} vs. H/T) at $T = 2$, 5, 10 K for tetraradical **6** in THF. The curves corrrespond to the Brillouin functions for $S = {}^3/_2$, 2, ${}^5/_2$.

Therefore, the high-spin species that correspond to the center $\Delta m_s = 2$ peaks are ground states or, less likely, there are near degeneracies between the low- and high-spin states.[5c]

The resolved ESR spectra, $\Delta m_s = 1$ and 2 for **4** and $\Delta m_s = 1$ for **5**, suggest that the observed high-spin species are quintets. Although the ESR spectrum for **6** cannot be definitely assigned at this time, low intensity of the center peak in the $\Delta m_s = 1$ spectrum of **6** (and **5**) suggests a small amount of the half-integral spin impurities.[20] Therefore, **5** and **6** in solution are excellent candidates for bulk magnetization studies using SQUID which should establish the spin values and resolve the question of the possible degeneracy between the spin states.

5 and **6** (~0.015 M) in THF are used for SQUID measurements.[4a] In the normalized plots of magnetization (M/M_{sat}) vs. the ratio of the magnetic field and temperature (H/T), the experimental points at $T = 2$, 5, 10 K (**6**) and $T = 2$, 5, 10, 20 K (**5**) are compared to the Brillouin curves, which correspond to the theoretically predicted behavior for a paramagnet of a given spin (S).[22] For **6**, the experimental points fall between the $S = 2$ and ${}^3/_2$ Brillouin curves; the $T = 10$ and 2 K points are close to the $S = 2$ and ${}^3/_2$ curves, respectively (Figure 5). Similar results are obtained for **5**.[26] The slight temperature dependence of the magnetization data may be caused by antiferromagnetic interactions; presumably, their origin is intermolecular.[4a] We conclude that tetraradicals **4**, **5**, and **6** possess quintet ground states.

UV–Visible Spectroscopy and Electrochemistry. Solutions of triradical **3** and tetraradical **6** are prepared by dissolving solid tri- and tetraradicals in THF. The UV–vis spectrum for triradical **3** and tetraradical **6** possesses an intense band at $\lambda_{max} = 350$ nm. Both λ_{max} and shape of the band are similar to those of the homologous triplet diradical.[14a] Therefore, the extension of π-conjugation does not perturb the electronic spectra of 1,3-connected polyradicals. For the related carbopolyanions, which differ from polyradicals by electron occupation of their nonbonding MOs, analogous behavior was found.[15a]

Electrochemcial studies of **3** in THF with tetrabutylammonium perchlorate (TBAP) as supporting electrolyte are done at low temperature (195–200 K). In cyclic voltammetry (CV), three reversible waves are observed at $E_p = -1.36$, -1.43, and -1.86 V. The currents for each wave in the steady-state CV (e.g., 0.001 V/s at 100-μm-diameter electrode) are in the ratio of 1:1:1. The

(22) Henry, W. E. *Phys. Rev.* **1952**, *88*, 559; ref 10.

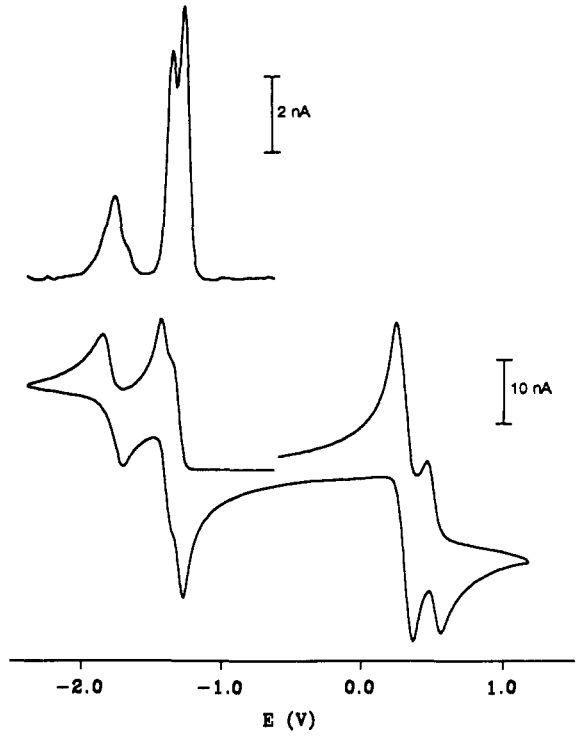

Figure 6. Voltammetry for triradical **3** in THF/TBAP at 200 K. Top: Differential pulse voltammogram. Bottom: Cyclic voltammogram with scan rate = 100 mV/s. Potentials are given vs. SCE using ferrocene (0.510 V) as the reference.

chronoamperometric limiting currents, which correspond to the potential steps including either the first two waves or all three waves, are in agreement with the steady-state CV measurements. This suggests that one-electron waves are observed and, therefore, they may be assigned to reduction of triradical **3** to the diradical anion, radical dianion, and trianion. Similarly, in differential pulse voltammetry (DPV) and square-wave voltammetry, three peaks are well resolved in the −1.2 to −1.9 V potential range.[23] Oxidation of triradical (two waves in the 0.2–0.5 V range) is only partially reversible at our experimental conditions (Figure 6).

Magnetic Studies in the Solid State. Solid triradical **3** and tetraradical **6** are examined using a SQUID magnetometer.

For **3**, the magnetization data at $T = 5$ and 10 K follow the $S = {}^3/_2$ Brillouin curve as expected for a paramagnet in a quartet state (Figure 7). At lower temperatures, the onset of weak antiferromagnetic interactions is observed as indicated by the $T = 2$ K magnetization data which approach the $S = 1$ Brillouin curve. Next, the product of magnetic susceptibility (χ) and temperature (T) is plotted versus temperature (T) at a constant applied magnetic field ($H = 0.5$, 0.05 T) (Figure 7, insert). Above $T = 10$ K, the χT product is approximately constant which indicates paramagnetic behavior; at low temperature, a downward turn is observed which suggests onset of antiferromagnetic interactions. The Curie–Weiss analysis of the magnetic susceptibility data, $\chi = C/(T - \theta)$, at $T > 50$ K gives C that corresponds to a magnetic moment, $\mu_{eff} = 3.9\ \mu_B$, which is in agreement with the theoretical spin-only value for a quartet ($S = {}^3/_2$) state of $\mu_{eff} = 3.93\ \mu_B$.[24]

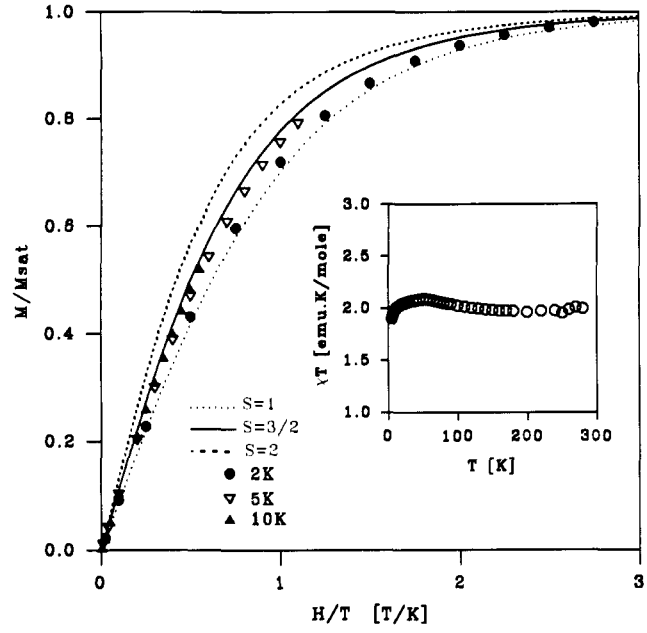

Figure 7. Normalized plots of magnetization vs. ratio of magnetic field and temperature (M/M_{sat} vs. H/T) at $T = 2$, 5, 10 K for solid triradical **3**. The curves correspond to the Brillouin functions for $S = 1$, ${}^3/_2$, 2. Insert: Plot of the product of magnetic susceptibility and temperature vs. temperature (χT vs. T) at constant magnetic field, $H = 0.5$ T.

The SQUID data indicate that **3** is a quartet ground state with negligible amounts of paramagnetic and diamagnetic impurities; the weak antiferromagnetic interactions observed in the liquid helium temperature range are most likely intermolecular. Furthermore, the flatness of the χT vs. T plot in the 10–300 K temperature range indicates that the thermal population of the low-spin excited states is undetectable even at ambient temperature; that is, the quartet ground state is separated by >1 kcal mol^{-1} from the low-spin excited states.

For tetraradical **6**, magnetization (M/M_{sat} vs. H/T) and magnetic susceptibility (χT vs. T, χ vs. $C/(T = \theta)$; $H = 0.5$, 0.05 T) data closely resemble those for triradical **3**;[26] e.g., $S \approx {}^3/_2$ ($T = 5$, 10 K), $S < {}^3/_2$ ($T = 2$ K), $\mu_{eff} = 3.9\ \mu_B$, $\theta = -2.1$ K.[24c] The ESR spectra indicate that the lower than expected average spin values and magnetic moment may be explained by the presence of paramagnetic impurities in solid **6**; when solid **6** is dissolved in 2-MeTHF, the ESR spectral pattern characteristic of **6** is obtained but the center peak, which may correspond to the odd-integral spin impurities, is by far dominant in the spectrum. Similarly to **3**, because of the flatness of the χT vs. T plot in the 10–280 K temperature range for **6**, it is concluded that the quintet ground state is at least 1 kcal mol^{-1} below the low-spin excited states.

Conclusion

1,3-Connected poly(arylmethyl) tri- and tetraradicals possess quartet and quintet ground states, respectively. The most sterically hindered tri- and tetraradicals, which can be studied up to ambient temperature in the solid state, show large preference (>1 kcal mol^{-1}) for the high-spin ground state. Although steric hindrance has to cause significant out-of-plane twisting in the π-conjugated system of **3** and **6**, it does not prevent strong intramolecular ferromagnetic coupling.

The next step toward a "single-molecule" magnet will require synthesis of very-high-spin, stable, and controlled-molecular-shape polyradicals. Steric hindrance can make polyradicals stable and may help to define their molecular shape;[8] such molecular engineering should not adversely affect strong ferromagnetic coupling. Therefore, 1,3-connected poly(arylmethyl) polyradicals are one of the most exciting precursors for organic magnets.

Experimental Section

Preparation of Triradicals (1-3) and Tetraradicals (4-6). A. Solutions of Polyradicals in THF. a Lithium piece (excess amount) was added to

(23) The most negative DPV peak at $E_{DPV} = -1.79$ V is broadened at the less negative potential side; similar distortion of the wave shape is observed in CV at slow scan rates. This may suggest the presence of another electroactive species.

(24) (a) The positive θ value of 3.5 K for solid **3** reflects slightly upward slope in the χT vs T plot from $T = 200$ to 50 K. Such minute variations of slope, which might originate in weak magnetic interactions or small contamination of the magnetometer chamber with oxygen, are sometimes found in solids of organic radicals, e.g., ref 14a and references therein. (b) The quality of the magnetic data, which are obtained by SQUID on air-sensitive and weakly magnetic solid samples such as **3** and **6**, is limited by the complexity of the sample preparation. (c) The θ values for solid **3** and **6** should be viewed as fitting parameters.

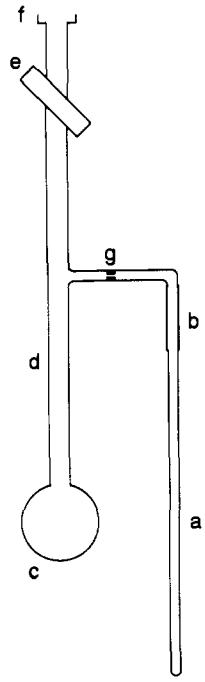

Figure 8. Vessel for preparation of polyradicals at low temperature: (a) 4-mm o.d. quartz ESR tube; (b) 5-mm o.d. glass-to-quartz seal; (c) 10-mL volume bulb; (d) 9-mm o.d. glass tubing; (e) Kontes 4-mm high-vacuum stopcock; (f) Fisher-Porter 9-mm solv-seal glass joint; (g) 1–2 mm i.d. constriction.

a solution of tri- or tetraether (0.02–0.01 mmol) in THF (0.5–0.6 mL). The reaction mixture was stirred for 2–7 days in a glovebox. The solution of carbanion was transferred to the oxidation vessel with a syringe. (An additional 0.2 mL of THF was used to complete the transfer.) The oxidation vessel is shown in Figure 8. Iodine (1.5 or 2 equiv) was added under a stream of argon to a stirred solution of tri- or tetraanion at ≤195 K on a vacuum line.

B. Samples in 2-MeTHF/THF for ESR Spectroscopy. The polyradical in THF at 195 K was placed under vacuum for several minutes. Subsequently, the THF solution was frozen using liquid N_2 and 2-MeTHF (5–6 mL) was transferred from purple Ph_2CO/Na over a vacuum line. The resultant mixture was melted at 195 K and, after the vacuum stopcock was closed, the oxidation vessel (Figure 8) was immersed up to the vacuum stopcock in a 160 K bath (EtOH/liquid N_2 slush). After the upper part of the vessel was coated with a thick layer of frozen EtOH, the oxidation vessel was *briefly* withdrawn from the bath and tilted to transfer a small amount of polyradical in 2-MeTHF/THF to the ESR tube part of the vessel. After the vessel was immersed in a 160 K bath or, better, liquid N_2, the repetitive application of temperature gradients to the wall of the vessel allows for complete transfer of the solution into the bottom part of the ESR tube. The ESR tube is flame sealed and stored in liquid N_2.

C. Samples in THF for SQUID Magnetometry. The polyradical in THF was prepared as described in procedure A above with the following difference; the carbanion was transferred to the oxidation vessel (Figure 8) that already contained pure THF in the ESR tube (65-mm height at ambient temperature). After the oxidation was completed, the solution of polyradical was kept at 195 K under argon. The vacuum stopcock was closed and pure THF in the ESR tube was frozen with liquid N_2. Subsequently, the oxidation vessel was immersed in a 160 K bath (EtOH/liquid N_2 slush) for 1–2 min. After the upper part of the vessel was coated with a thick layer of frozen EtOH, the oxidation vessel was *briefly* withdrawn from the bath and tilted to transfer a small amount of polyradical in THF to the constriction in the tube connecting the ESR tube to the rest of the vessel. After the vessel was immersed in a 160 K bath or, better, liquid N_2, the repetitive application of temperature gradients to the wall of the vessel allowed for complete transfer of the solution onto the frozen THF in bottom part of the ESR tube. After a sample band of 3-mm-height was formed, the vessel was placed under vacuum (the ESR tube has to be immersed in liquid N_2) and the ESR tube was filled with pure THF (60-mm height) above the frozen sample band by vacuum transfer. The ESR tube was flame sealed about 60 mm above the frozen THF and stored in liquid N_2.

D. Solid Triradical 3 and Tetraradical 6. A double-tube recrystallizer, which was equipped with PTFE high-vacuum stopcocks and a glass frit (4–8 μm), was loaded with the corresponding trianion or tetraanion (~0.06 mmol) in THF (1.2 mL) in the glovebox. THF was removed under vacuum and Me_2O (1.0–1.5 mL) was vacuum transferred from purple Ph_2CO/Na. Iodine (1.5 or 2 equiv) was added under a stream of argon to a stirred suspension of tri- or tetraanion in Me_2O at 195 K. Because of poor solubility for both the carbanions and the polyradicals in Me_2O at 195 K, temperature was occasionally raised above 195 K but kept well below the boiling point of Me_2O at ambient pressure of argon. After the oxidation, Me_2O was removed under vacuum at 195 K. The remaining solid residue was repeatedly washed with degassed MeOH. The yellow-green solid was dried under vacuum overnight (5×10^{-4} Torr) at ambient temperature and then stored in the glovebox refrigerator (243 K).

ESR Spectroscopy. Bruker 200D SRC and 200D instruments were used to obtain X-band ESR spectra. The 200D instrument was equipped with a 90 dB bridge and the power meter. Temperatures in the 300–100 K range were controlled by a nitrogen flow system (Varian); temperatures were measured using a thermocouple. Temperatures in the 80–4 K range were controlled and measured using an Oxford Instruments ESR900 cryostat. High vacuum ($p < 1 \times 10^{-5}$ Torr, cold cathode gauge) was maintained in the cryostat shield with a liquid nitrogen trapped oil diffusion/rotary pump set; flexible stainless steel Cajon tubing connected the pumps to the cryostat.

The ESR intensities for Curie plots in the 4–80 K range were obtained at identical instrument settings except for the receiver gain for a given sample; several spectra were recorded at each temperature at one or two gain settings. The power attenuation settings were increased by at least 10 dB compared to the setting corresponding to the maximum peak-to-peak height for the measured resonance at 4 K. The temperatures were stepped up from 4 to 80 K (or 65 K) and then stepped down to the 10–20 K temperature range.

SQUID. Magnetometry of polyradicals in frozen solutions and solid state have been described.[4a,14a] Preparation of the frozen solution samples for SQUID is detailed in the preceding text. In this work both solid triradical and solid tetraradical were measured using two methods of sample preparation, method A[14a] and method B, which is based upon the following sequence: (1) the ESR quartz tube was loaded with molten wax and after solidification the wax was compressed with a warm glass rod (the tube was filled with the wax from the bottom to the height of 60 mm); (2) the solid polyradical (ca. 15 mg) was tightly packed on the surface of the wax, (3) a piece of solid wax, which tightly fits the ESR quartz tube, was inserted before sealing the tube with molten wax (the height of the wax layer above the solid polyradical was about 60 mm, after compression). The quartz tube was then mounted to the SQUID sample holder using heat-shrink tubing. In method B, no correction for diamagnetism was applied. Although both method A and method B give identical results, method B is more suitable for this work because of good signal-to-noise in the 200–300 K temperature range. Standard numerical procedures were used to fit the magnetization data at $T = 2$ K to the Brillouin functions; both M_{sat} and S were varied. This M_{sat} was used for normalized magnetization plots at all temperatures.

Electrochemistry. Electrochemical measurements were carried out in a Vacuum Atmospheres aluminum glovebox using a PARC Model 270 electrochemistry system. All electrical cables were shielded and the glovebox was thoroughly grounded. The homemade electrochemical cell was placed (sliding fit) in the copper-block heat exchanger at the bottom of the Vacuum Atmospheres liquid nitrogen cold well. Temperature of the electrolyte was measured using a thermocouple probe which was inserted into the cell in a THF-filled thin-wall glass capillary (o.d. 1 mm). The control of the cooling rate and large heat volume of the copper block allowed for the control of temperature. Three electrodes were used: quasi-reference (Ag-wire), counter (Pt-foil), and working (Pt-disk either 100- or 10-μm diameter as supplied by BAS). The solution volume was 2 mL. The typical CV scan rate was 100 mV/s (for 100-μm-diameter electrode). Ferrocene (0.510 V vs SCE) was used as a reference.[25]

Acknowledgment. We gratefully acknowledge the National Science Foundation for the support of this research (CHEM-8912762 and CHE-9203918). We thank Professor Sy-Hwang Liou at the University of Nebraska for access to a SQUID magnetometer.

Supplementary Material Available: ESR spectra and SQUID data (10 pages). Ordering information is given on any current masthead page.

(25) Ferrocene: Diggle, J. W.; Parker, A. J. *J. Electrochem. Acta* **1973**, *18*, 976.

(26) See supplementary material.